

Beyond Sharing Weights for Deep Domain Adaptation

Artem Rozantsev, Mathieu Salzmann, Pascal Fua
{firstname.lastname}@epfl.ch

Computer Vision Laboratory, École Polytechnique Fédérale de Lausanne, Lausanne,
Switzerland

Abstract. Deep Neural Networks have demonstrated outstanding performance in many Computer Vision tasks but typically require large amounts of labeled training data to achieve it. This is a serious limitation when such data is difficult to obtain. In traditional Machine Learning, Domain Adaptation is an approach to overcoming this problem by leveraging annotated data from a *source domain*, in which it is abundant, to train a classifier to operate in a *target domain*, in which labeled data is either sparse or even lacking altogether. In the Deep Learning case, most existing methods use the same architecture with the same weights for both source and target data, which essentially amounts to learning domain invariant features. Here, we show that it is more effective to explicitly model the shift from one domain to the other. To this end, we introduce a two-stream architecture, one of which operates in the source domain and the other in the target domain. In contrast to other approaches, the weights in corresponding layers are related but *not shared* to account for differences between the two domains. We demonstrate that this both yields higher accuracy than state-of-the-art methods on several object recognition and detection tasks and consistently outperforms networks with shared weights in both supervised and unsupervised settings.

Keywords: Domain adaptation, object detection/recognition, deep learning.

1 Introduction

Deep Neural Networks [1, 2] have emerged as powerful tools that outperform traditional Computer Vision algorithms in a wide variety of tasks, but only when sufficiently large amounts of training data are available. This is a severe limitation in fields in which obtaining such data is either difficult or expensive. For example, this work was initially motivated by our need to detect drones against complicated backgrounds with a view to developing anti-collision systems. Because the set of possible backgrounds is nearly infinite, creating an extensive enough training database of representative real images proved to be very challenging.

Domain Adaptation [3] and Transfer Learning [4] have long been used to overcome this difficulty by making it possible to exploit what has been learned in one specific domain, for which enough training data is available, to effectively train classifiers in a related but different domain, where only very small amounts of additional annotations, or even none, can be acquired. Following the terminology of Domain Adaptation, we will refer to the domain in which enough annotated data is available as the *source domain* and the one with only limited amounts of such data, or none at all, as the *target*

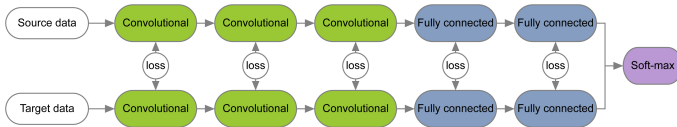


Fig. 1. Our two-stream architecture. One stream operates on the source data and the other on the target one. Their weights are *not* shared. Instead, we introduce loss functions that prevent corresponding weights from being too different from each other.

domain. In the drone case discussed above, the source domain can comprise synthetic images of drones, which can be created in arbitrary quantities, and the target domain a relatively small number of annotated real images. Again as in the domain adaptation literature, we will refer to this scenario as the *supervised* one. An even more difficult situation arises when there is absolutely no annotated data in the target domain. We will refer to this as the *unsupervised* scenario. In this paper, we will investigate both of the aforementioned scenarios.

Recently, Domain Adaptation has been investigated in the context of Deep Learning with promising results. The simplest approach involves fine-tuning a Convolutional Neural Network (CNN) pre-trained on the source data using labeled target samples [5, 6]. This, however, results in overfitting when too little target data is available. Furthermore, it is not applicable in the unsupervised case. To overcome these limitations, other works have focused on using both source and target samples to learn a network where the features for both domains, or their distributions, are related via an additional loss term [7–10]. To the best of our knowledge, all such methods use the same deep architecture with the same weights for both source and target domains. As such, they can be understood as attempts to make the features invariant to the domain shift, that is, the changes from one domain to the other.

In this paper, we postulate that imposing feature invariance might be detrimental to discriminative power. To verify this hypothesis, we introduce a different approach that explicitly models the domain shift by allowing the CNN weights to compensate for it. To this end, we rely on the two-stream architecture depicted by Fig. 1. One stream operates on the source domain and the other on the target one. Their weights are *not* shared. Instead, we introduce a loss function that is lowest when they are linear transformations of each other. In short, our approach models the domain shift by learning features adapted to each domain, but not fully independent, to account for the fact that both domains depict the same object categories.

Motivated by our drone detection application, we demonstrate the benefits of our approach on a Unmanned Aerial Vehicles (UAV) image dataset, consisting of a large amount of synthetic data and a small amount of real images. We show that our approach lets us successfully leverage the synthetic data. In particular, we can reach the same level of accuracy as a model trained on a large set of real data by using only 5-10% of real data in conjunction with synthetic examples. This could have a huge impact in many research areas, such as human pose estimation, where labeling new data is time-consuming and costly, but generating synthetic examples is relatively easy. Furthermore, to demonstrate the generality of our approach, we also apply it to two standard benchmark Domain Adaptation datasets, covering both the supervised and unsupervised scenarios and different network architectures. Our non-shared weight approach consis-

tently outperforms those that share all the weights and improves on the state-of-the-art in all cases.

2 Related work

In many practical applications, classifiers and regressors may have to operate on many kinds of related but visually different image data. The differences are often large enough for an algorithm that has been trained on one kind of images to perform badly on another. Therefore, new training data has to be acquired and annotated to retrain it. Since this is typically expensive and time-consuming, there has long been a push to develop Domain Adaptation techniques that allow re-training with minimal amounts of new data or even none. We review here briefly some recent trends, with a focus on Deep Learning based methods, which are most related to our work.

A natural approach to Domain Adaptation is to modify a classifier trained on the source data using the available labeled target data. This was done, for example, using SVM [11, 12], Boosted Decision Trees [13] and other classifiers [14]. In the context of Deep Learning, fine-tuning [5, 6] essentially follows this pattern. In practice, however, when little labeled target data is available, this often results in overfitting.

Another approach is to learn a metric between the source and target data, which can also be interpreted as a linear cross-domain transformation [15] or a non-linear one [16]. Instead of working on the samples directly, several methods involve representing each domain as one separate subspace [17–19]. A transformation can then be learned to align them [19]. Alternatively, one can interpolate between the source and target subspaces [17, 18]. In [20], this interpolation idea was extended to Deep Learning by training multiple unsupervised networks with increasing amounts of target data. The final representation of a sample was obtained by concatenating all intermediate ones. It is unclear, however, why this concatenation should be meaningful to classify a target sample.

Another way to handle the domain shift is to explicitly try making the source and target data distribution similar. While many metrics have been proposed to quantify the similarity between two distributions, the most widely used in the Domain Adaptation context is the Maximum Mean Discrepancy (MMD) [21]. The MMD has been used to re-weight [22, 23] or select [24] source samples such that the resulting distribution becomes as similar as possible to the target one. An alternative is to learn a transformation of the data, typically both source and target, such that the resulting distributions are as similar as possible in MMD terms [25–27]. In [28], MMD was used within a shallow neural network architecture. However, this method relied on SURF features [29] as initial image representation and thus only achieved limited accuracy.

Recently, using Deep Networks to learn features has proven effective at increasing the accuracy of Domain Adaptation methods. In [30], it was shown that using DeCAF features instead of hand-crafted ones mitigates the Domain Shift effects even without performing any kind of adaptation. However, performing adaptation within a Deep Learning framework was shown to boost accuracy further [31, 7–10]. For example, in [31], a Siamese architecture was introduced to minimize the distance between pairs of source and target samples, which requires training labels available in the *target* domain thus making the method unsuitable for unsupervised Domain Adaptation.

The MMD has also been used to relate the source and target data representations [7, 8] thus making it possible to avoid working on individual samples. In [9, 10], a loss term that encodes an additional classifier predicting from which domain each sample comes was introduced. This was motivated by the fact that, if the learned features are domain-invariant, such a classifier should exhibit very poor performance.

All these Deep Learning approaches rely on the same architecture with the same weights for both the source and target domains. In essence, they attempt to reduce the impact of the domain shift by learning domain-invariant features. In practice, however, domain invariance might very well be detrimental to discriminative power. As discussed in the introduction, this is the hypothesis we set out to test in this work by introducing an approach that explicitly models the domain shift instead of attempting to enforce invariance to it. We will see in the results section that this yields a significant accuracy boost over networks with shared weights.

3 Our Approach

In this section, we introduce our Deep Learning approach to Domain Adaptation. At its heart lies the idea that, for the model to adapt to different domains, the network weights should be related, yet different for each of the two domains. This constitutes a major difference between our approach and the competing ones discussed in Section 2. To implement this idea, we therefore introduce a two-stream architecture, such as the one depicted by Fig. 1. The first stream operates on the source data, the second on the target one, and they are trained jointly. While we allow the weights of the corresponding layers to differ between the two streams, we prevent them from being too far from of each other by introducing appropriately designed loss functions. Additionally we use the MMD between the learned source and target representations. This combination lets us encode the fact that, while different, the two domains are related.

More formally, let $\mathbf{X}^s = \{\mathbf{x}_i^s\}_{i=1}^{N^s}$ and $\mathbf{X}^t = \{\mathbf{x}_i^t\}_{i=1}^{N^t}$ be the sets of training images from the source and target domains, respectively, with $Y^s = \{y_i^s\}$ and $Y^t = \{y_i^t\}$ being the corresponding labels. To handle unsupervised target data as well, we assume, without loss of generality, that the target samples are ordered, such that only the first N_l^t ones have valid labels, where $N_l^t = 0$ in the unsupervised scenario. Furthermore, let θ_j^s and θ_j^t denote the parameters, that is, the weights and biases, of the j^{th} layer of the source and target streams, respectively. We train the network by minimizing a loss function of the form

$$L(\theta^s, \theta^t | \mathbf{X}^s, Y^s, \mathbf{X}^t, Y^t) = L_s + L_t + L_w + L_{MMD}, \quad (1)$$

$$L_s = \frac{1}{N^s} \sum_{i=1}^{N^s} c(\theta^s | \mathbf{x}_i^s, y_i^s) \quad (2)$$

$$L_t = \frac{1}{N_l^t} \sum_{i=1}^{N_l^t} c(\theta^t | \mathbf{x}_i^t, y_i^t) \quad (3)$$

$$L_w = \lambda_w \sum_{j \in \Omega} r_w(\theta_j^s, \theta_j^t) \quad (4)$$

$$L_{MMD} = \lambda_u r_u(\theta^s, \theta^t | \mathbf{X}^s, \mathbf{X}^t), \quad (5)$$

where $c(\theta \cdot | \mathbf{x}_i, y_i)$ is a standard classification loss, such as the logistic loss or the hinge loss. $r_w(\cdot)$ and $r_u(\cdot)$ are the weight and unsupervised regularizers discussed below. The first one represents the loss between corresponding layers of the two streams. The second encodes the MMD measure and favors similar distributions of representations of source and target data. These regularizers are weighted by coefficients λ_w and λ_u , respectively. In practice, we found our approach to be robust to the specific values of these coefficients and we set them to 1 in all our experiments. Ω denotes the set of indices of the layers whose parameters are not shared. This set is problem-dependent and, in practice, can be obtained from validation data, as demonstrated in our experiments.

Weight regularizer. While our goal is to go beyond sharing the layer weights, we still believe that corresponding weights in the two streams should be related. This models the fact that the source and target domains are related, and prevents overfitting in the target stream, when only very few labeled samples are available. Our weight regularizer $r_w(\cdot)$ therefore represents the distance between the source and target weights in a particular layer. The simplest choice would be the L_2 norm $\|\theta_j^s - \theta_j^t\|_2^2$. This, however, would penalize even small differences between the weights and makes the whole system too rigid. To add more flexibility, we therefore use the exponential loss function and write

$$r_w(\theta_j^s, \theta_j^t) = \exp(\|\theta_j^s - \theta_j^t\|^2) - 1. \quad (6)$$

While the exponential loss of Eq. 6 gives more flexibility than the L_2 loss, it still tends to keep the weights of both streams very close to each other, which might be too restrictive when the domains differ significantly. We therefore propose to further relax this prior by allowing the weights in one stream to undergo a linear transformation. We express this as

$$r_w(\theta_j^s, \theta_j^t) = \exp(\|a_j \theta_j^s + b_j - \theta_j^t\|^2) - 1, \quad (7)$$

where a_j and b_j are scalar parameters that encode the linear transformation. These parameters are different for each layer $j \in \Omega$ and are learned at training time together with all other network parameters. While simple, this approach lets us model parameter transformations such as those depicted by Fig. 2 and has proven to be effective in practice. For example, this parametrization can account for global illumination changes in the first layer of the network. We have tried replacing the simple linear transformation of Eq. 7 by more sophisticated ones, such as quadratic or more complicated linear transformations. However, this has not resulted in any performance improvement.

Unsupervised regularizer. In addition to regularizing the weights of corresponding layers in the two streams, we also aim at learning a final representation, that is, the features before the classifier layer, that is domain invariant. To this end, we introduce a regularizer $r_u(\cdot)$ designed to minimize the distance between the distributions of representations of the source and target data. Following the popular trend in Domain Adaptation [32, 7], we rely on the Maximum Mean Discrepancy (MMD) [21] to encode this distance.

As the name suggests, given two sets of data, the MMD measures the distance between the mean of the two sets after mapping each sample to a Reproducing Kernel

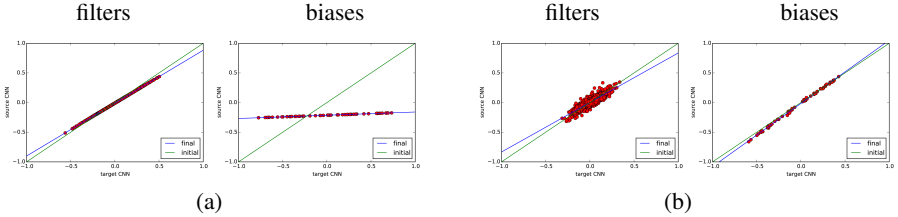


Fig. 2. Correlation between weights of the corresponding first convolutional layer of CNN_t and CNN_s , regularized by L_2 (a) and exponential norm, defined by Eq. 7 (b). The red dots denote the correlation between the corresponding layer parameters. The green line shows the initial estimate for the linear transformation and the blue line illustrates its final estimate after the training process. (best seen in color)

Hilbert Space (RKHS). In our context, let $\mathbf{f}_i^s = \mathbf{f}_i^s(\theta^s, \mathbf{x}_i^s)$ be the feature representation at the last layer of the source stream, and similarly for the target stream. The squared MMD between the source and target domains can be expressed as

$$\text{MMD}^2(\{\mathbf{f}_i^s\}, \{\mathbf{f}_j^t\}) = \left\| \frac{1}{N^s} \sum_{i=1}^{N^s} \phi(\mathbf{f}_i^s) - \frac{1}{N^t} \sum_{j=1}^{N^t} \phi(\mathbf{f}_j^t) \right\|^2, \quad (8)$$

where $\phi(\cdot)$ denotes the mapping to RKHS. In practice, this mapping is typically unknown. However, expanding Eq. 8 yields

$$\text{MMD}^2(\{\mathbf{f}_i^s\}, \{\mathbf{f}_j^t\}) = \sum_{i,i'} \frac{\phi(\mathbf{f}_i^s)^T \phi(\mathbf{f}_{i'}^s)}{(N^s)^2} - 2 \sum_{i,j} \frac{\phi(\mathbf{f}_i^s)^T \phi(\mathbf{f}_j^t)}{N^s N^t} + \sum_{j,j'} \frac{\phi(\mathbf{f}_j^t)^T \phi(\mathbf{f}_{j'}^t)}{(N^t)^2}. \quad (9)$$

By using the kernel trick, the inner products can be replaced by kernel values. This lets us rewrite our regularizer as

$$r_u(\theta^s, \theta^t | \mathbf{X}^s, \mathbf{X}^t) = \sum_{i,i'} \frac{k(\mathbf{f}_i^s, \mathbf{f}_{i'}^s)}{(N^s)^2} - 2 \sum_{i,j} \frac{k(\mathbf{f}_i^s, \mathbf{f}_j^t)}{N^s N^t} + \sum_{j,j'} \frac{k(\mathbf{f}_j^t, \mathbf{f}_{j'}^t)}{(N^t)^2}, \quad (10)$$

where the dependency on the network parameters comes via the \mathbf{f}_i^s s, and where $k(\cdot, \cdot)$ is a kernel function. In practice, we make use of the standard RBF kernel $k(u, v) = \exp(-\|u - v\|^2 / \sigma_2)$, with σ_2 being the bandwidth of the kernel. In all our experiments, we found our approach to be insensitive to the choice of σ_2 and we therefore set it to 1.

Training. To learn the model parameters, we first pre-train the source stream using the source data only. We then simultaneously optimize the weights of both streams according to the loss of Eqs. 2-5 using both source and target data, with the target stream weights initialized from the pre-trained source weights. Note that this also requires initializing the linear transformation parameters of each layer, a_j and b_j for all $j \in \Omega$. We initialize these values to $a_j = 1$ and $b_j = 0$, thus encoding the identity transformation. All parameters are then learned jointly using backpropagation with the AdaDelta algorithm [33]. Note that we rely on mini-batches, and thus in practice use all the terms of our loss over these mini-batches rather than over the entire source and target datasets.

Depending on the task, we use different network architectures, to provide a fair comparison with the baselines. For example, for digit classification we rely on the standard network structure of [34] for each stream, and, for the *Office* benchmark, we adopt the AlexNet [35] architecture, as was done in [7].

4 Experimental Results

In this section, we show the benefits of our approach in both the supervised and unsupervised scenarios using different network architectures. Since our motivating application was drone detection, we first thoroughly evaluate our method for this task. We then demonstrate that it generalizes well to other problems by testing it on standard benchmark datasets.

4.1 Leveraging Synthetic Data for Drone Detection

As drones and UAVs become ever more numerous in our skies, it will become increasingly important for them to see and avoid colliding with each other. Unfortunately, training videos are scarce and do not cover a wide enough range of possible shapes, poses, lighting conditions, and backgrounds against which they can be seen. However, it is relatively easy to generate large amounts of synthetic examples, which can be used to supplement a small number of real images and increase the detection accuracy [36]. We show here that our approach allows us to exploit these synthetic images more effectively than other state-of-the-art Domain Adaptation techniques.

Dataset and Evaluation Setup. We used the approach of [36] to create a large set of synthetic examples. We also collected three sets of real images, such as those depicted by Fig. 3, which we used for training, validation, and testing, respectively. In our experiments, we treat the synthetic images as samples from the source domain and the real ones as samples from the target domain.

We report results using two versions of this dataset, which we refer to as *UAV-200 (small)* and *UAV-200 (full)*. Their sizes are given in Table 1. They only differ in the number of synthetic and negative samples used at training and testing time. The ratio of positive to negative samples in the first dataset is more balanced than in the second one. For *UAV-200 (small)*, we therefore express our results in terms of *accuracy*, which is commonly used in Domain Adaptation and can be computed as

$$\text{Accuracy} = \frac{\# \text{ correctly classified examples}}{\# \text{ all examples}}. \quad (11)$$

Using this standard metric facilitates the comparison against the baseline methods whose publicly available implementations only output classification accuracy.

In real detection tasks, however, the training datasets are typically quite unbalanced, since one usually encounters many negative windows for each positive one. *UAV-200 (full)* reflects this more realistic scenario, in which the accuracy metric is poorly-suited. For this dataset, we therefore compare various approaches in terms of *precision-recall*. Precision corresponds to the number of true positives detected by the algorithm

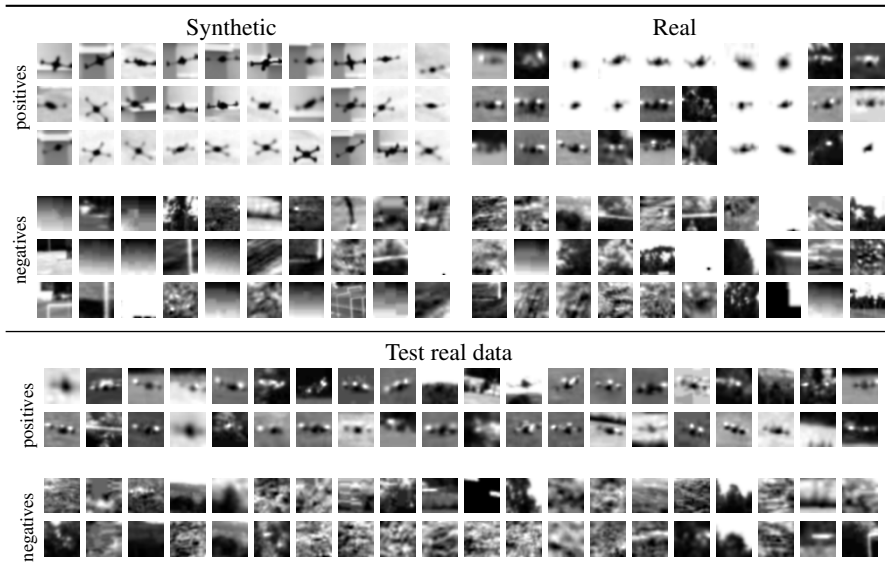


Fig. 3. Our UAV dataset. Top: Synthetic and real training examples. **Bottom:** Real samples from the test dataset.

Dataset	Training			Validation		Testing	
	Pos		Neg	Pos	Neg	Pos	Neg
	(Real)	(Synthetic)	(Real)	(Real)	(Real)	(Real)	(Real)
UAV-200 (full)	200	32800	190000	500	1500	3100	135000
UAV-200 (small)	200	1640	9500	500	1500	3100	6750

Table 1. Statistics of our two UAV datasets. Note that *UAV-200 (small)* is more balanced than *UAV-200 (full)*.

divided by the total number of detections. Recall is the number of true positives divided by the number of test examples labeled as positive. Additionally, we report the *Average Precision (AveP)*, which is computed as $\int_0^1 p(r) dr$, where p and r denote precision and recall, respectively.

For both datasets, we follow the supervised Domain Adaptation scenario. In other words, training data is available with labels for both source and target domains. Testing is then done on the images from the test data, as described in Table 1.

Network Design. Since drone detection is a relatively new problem, there is no generally accepted network architecture, and we had to design our own. As illustrated by Fig. 1, our network consists of two streams, one for the synthetic data and one for the real data. Each stream is a CNN that comprises three convolutional and max-pooling layers, followed by two fully-connected ones. The classification layer encodes a hinge loss, which was shown to outperform the logistic loss in practice [37, 38].

Some pairs of layers in the two streams share their weights while others do not. To identify what the optimal arrangement should be, as well as which loss function should

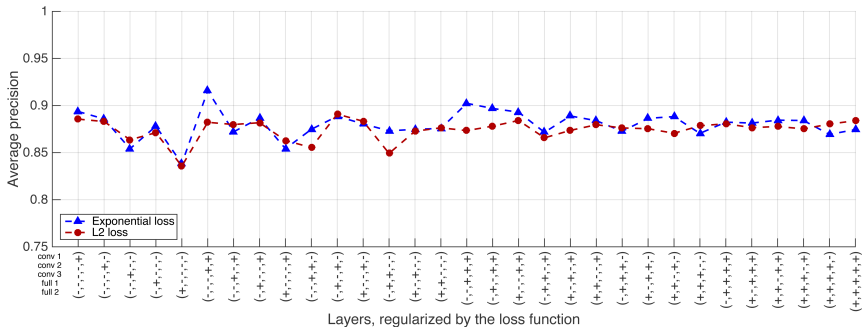


Fig. 4. Evaluation of the best network architecture. The x -axis denotes the network configuration, where a ‘+’ sign indicates that the corresponding network layers are regularized with a loss function and a ‘-’ sign that the weights are shared for the corresponding layers. We show the results of applying different loss functions: L_2 norm (red circles) and exponential loss Eq. 7 (blue triangles). These experiments were performed on the validation data of *UAV-200 (full)*. (best seen in color)

be employed between the non-shared layers, we trained different models corresponding to all possible combinations and evaluated them on the validation data. Fig. 4 depicts the results. In this figure, the + and - signs indicate whether the weights are stream-specific or shared. We can see that using the exponential loss to connect the layers that do not share their weights typically yields better accuracy than using the L_2 norm. The best performance overall is obtained when the first two convolutional layers are connected by an exponential loss function and the others share their weights. Our understanding is that, even though the synthetic and real images feature the same objects, they differ in appearance, which is mostly encoded by the first network layers. Thus, allowing the weights of the streams to differ in these layers lets each network better adapt to its domain. In any event, we used this architecture in the remainder of our drone detection experiments.

Evaluation. We first compare our approach to other Domain Adaptation methods on *UAV-200 (small)*. As can be seen in Table 2, it significantly outperforms many state-of-the-art baselines in terms of accuracy. In particular, we believe that outperforming DDC [7] goes a long way towards validating our hypothesis that modeling the domain shift is more effective than trying to be invariant to it. This is because, as discussed in Section 2, DDC relies on minimizing the MMD loss between the learned source and target representations much as we do, but uses a single stream for both source and target data. In other words, except for the non-shared weights, it is the method closest to ours. Note, however, that the original DDC paper used a slightly different network architecture than ours. To avoid any bias, we therefore modified this architecture so it matches ours in our own DDC implementation.

We then turn to the complete dataset *UAV-200 (full)*. In this case, the baselines whose implementations only output accuracy values become less relevant because it is not a good metric for unbalanced data. We therefore compare our approach against DDC [7], which we found to be our strongest competitor in the previous experiment, and against

	Accuracy
ITML [15]	0.60
ARC-t assymmetric [16]	0.55
ARC-t symmetric [16]	0.60
HFA [39]	0.75
DDC [7]	0.89
Ours	0.92

Table 2. Comparison to other domain adaptation techniques on the *UAV-200 (small)* dataset.

	AveP (Average Precision)
<i>CNN (trained on Synthetic only (S))</i>	0.314
<i>CNN (trained on Real only (R))</i>	0.575
<i>CNN (pre-trained on S and fine-tuned on R):</i>	
<i>Loss: L_t</i>	0.612
<i>Loss: $L_t + L_w$ (with fixed source CNN)</i>	0.655
<i>CNN (pre-trained on S and fine-tuned on R and S):</i>	
<i>Loss: $L_s + L_t$ [36]</i>	0.569
DDC [7] (<i>pre-trained on S and fine-tuned on R and S</i>)	0.664
<i>Our approach (pre-trained on S and fine-tuned on R and S)</i>	
<i>Loss: $L_s + L_t + L_w$</i>	0.673
<i>Loss: $L_s + L_t + L_{MMD}$</i>	0.711
<i>Loss: $L_s + L_t + L_w + L_{MMD}$</i>	0.757

Table 3. Comparing our method against baselines approaches on the *UAV-200 (full)* dataset. As discussed in Section 3, the terms L_s , L_t , L_w , and L_{MMD} correspond to the elements of the loss function, defined in Eqs. 2, 3, 4, 5, respectively.

the Deep Learning approach of [36], which also tackled the drone detection problem. We also turn on and off some of our loss terms to quantify their influence on final performance. We give the results in Table 3. In short, all the loss terms contribute to improving the AveP of our approach, which itself outperforms all the baselines by large margins. More specifically, we get a 10% boost over DDC and a 20% boost over using real data only. By contrast, simply using real and synthetic examples together, as was done in [36], does not really yield much improvement. Interestingly, allowing the weights of both streams to be independent while the outputs of their last fully-connected layers are regularized with an MMD loss (*Our approach: Loss: $L_s + L_t + L_{MMD}$*) achieves lower accuracy than our approach, which regularizes the weights of both streams. We attribute this to overfitting of the target stream to the target data.

Influence of the Number of Real and Synthetic Samples. Using synthetic data in the UAV detection scenario is motivated by the fact that it is hard and time consuming to collect large amounts of real data. We therefore evaluate the influence of the ratio of synthetic to real data. To this end, we first fix the number of synthetic samples to 32800, as in *UAV-200 (full)* and vary the amount of real positive samples from 200 to 5000. The results of this experiments are reported in Fig. 5(a), where we again compare

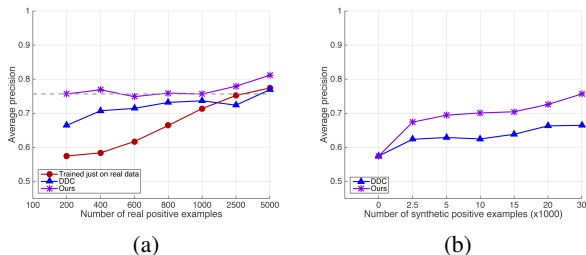


Fig. 5. Influence of the ratio of synthetic to real data. (a) AveP of our approach (violet stars), DDC (blue triangles), and training using real data only (red circles) as a function of the number of real samples used given a constant number of synthetic ones. (b) AveP of our approach (violet stars) and DDC (blue triangles) as a function of the number of synthetic examples used given a small and constant number of real one. (best seen in color)

our approach to DDC [7] and to the same CNN model trained on the real samples only. Our model always outperforms the one trained on real data only. This suggests that it remains capable of leveraging the synthetic data, even though more real data is available, which is not the case of DDC. More importantly, looking at the leftmost point on our curve shows that, with only 200 real samples, our approach performs similarly to, and even slightly better than, a model trained using 2500 real samples. In other words, one only needs to collect 5-10% of labeled training data to obtain good results with our approach, which, we believe, can have a significant impact in practical applications.

Fig. 5(b) depicts the results of a second experiment in which we fixed the number of real samples to 200 and increased the number of synthetic ones from 0 to 32800. Note that the AveP of our approach steadily increases as more synthetic data is used. DDC also improves but we systematically outperform it except when we use no synthetic samples, in which case both approaches reduce to a CNN trained on real data only.

4.2 Evaluation on Standard Classification Benchmarks

To demonstrate the generality of our approach, we further evaluate it on two standard domain adaptation benchmarks for image classification, one to test the supervised scenario and the other the unsupervised one. Following standard practice, we express our results in terms of *accuracy*, as defined in Eq. 11.

Supervised domain adaptation using the Office dataset. The *Office* dataset [15] comprises three different sets of images (Amazon, DSLR, Webcam) featuring 31 classes of objects. Fig. 6 depicts some images from the three different domains of the *Office* dataset. For our experiments, we used the evaluation protocol proposed in [15], which corresponds to the supervised scenario. Specifically, following [15], we used the labels of 20 randomly sampled images for each class for the Amazon domain and 8 labeled images per class for the DSLR and Webcam domains, when used as source datasets. For the target domain, we only used 3 randomly selected labeled images per class. The rest of the dataset, however, was used as unlabeled data for the calculation of the MMD loss of Eq. 5.

Fig. 7(a) illustrates the network architecture we used for this experiment. Each stream corresponds to the standard AlexNet CNN [35] with the additional adaptation

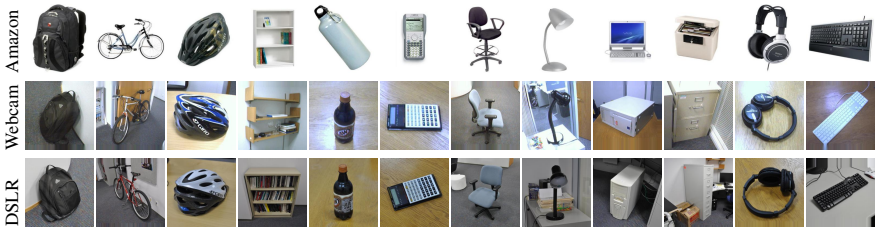


Fig. 6. Some examples from three domains in the Office dataset.

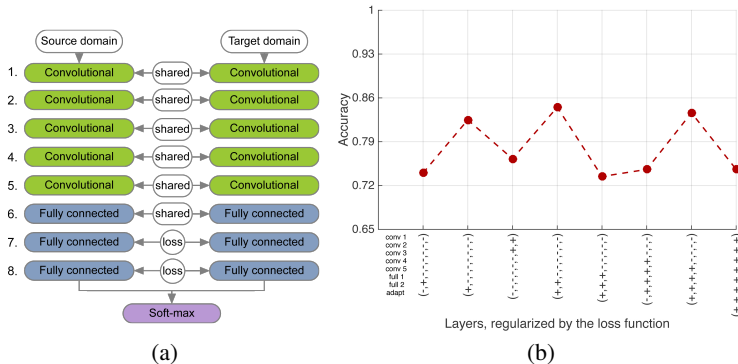


Fig. 7. Office dataset. (a) Our network architecture that proved to be best based on experiments on the validation set. (b) Several experiments on the validation set. On the x -axis we briefly describe the configuration that we use. For each layer ‘+’ denotes that the weights of the network are *not* shared, while ‘-’ means that corresponding layers share weights.

layers proposed in the DDC model of [7]. As in [7], we start with the pre-trained model and fine tune it. However, instead of forcing the weights of both streams to be shared, we allow them to deviate from each other and regularize this deviation using the loss function introduced in Section 3. To identify which layers should *not* share their weights and which ones should, we used a validation set consisting of 5 examples per object category in the *Amazon* \rightarrow *Webcam* domain adaptation task. Fig. 7(b) depicts some of the results of this validation procedure. As we can see, not sharing the last two fully-connected layers achieves the highest accuracy on this subset. Note that we only performed this validation on the *Amazon* \rightarrow *Webcam* task and used the same architecture for the other tasks reported below.

In Table 4, we compare our approach against other Domain Adaptation techniques on the three commonly-reported source/target pairs. It outperforms them on almost all pairs. More importantly, the comparison against DDC confirms that allowing the weights not to be shared increases accuracy.

Unsupervised domain adaptation using MNIST-USPS. The *MNIST* [34] and *USPS* [41] datasets for digit classification both feature 10 different classes of images corresponding to the 10 digits. They have recently been employed for the task of Domain Adaptation [42].

For this experiment, we used the evaluation protocol of [42], which involves randomly selecting of 2000 images from *MNIST* and 1800 images from *USPS* and using them interchangeably as source and target domains. As in [42], we work in the unsuper-

	Accuracy			
	A \rightarrow W	D \rightarrow W	W \rightarrow D	Average
GFK [18]	0.464	0.613	0.663	0.530
SA [19]	0.450	0.648	0.699	0.599
DA-NBNN [40]	0.528	0.766	0.762	0.685
DLID [20]	0.519	0.782	0.899	0.733
DeCAF ₆ +T [30]	0.807	0.948	-	-
DaNN [28]	0.536	0.712	0.835	0.694
DDC [7]	0.841	0.954	0.963	0.919
Ours	0.876	0.949	0.988	0.938

Table 4. Comparison to other domain adaptation techniques on the Office standard benchmark. We evaluate on all 31 categories, according to the standard evaluation protocol, described in [15].

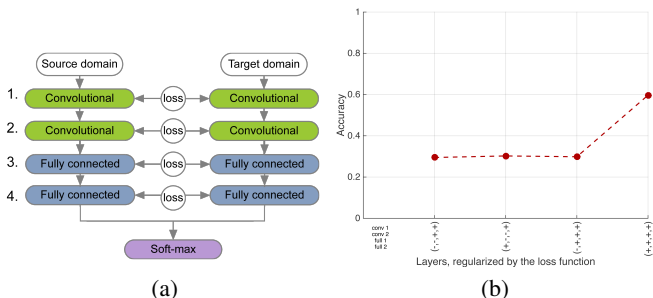


Fig. 8. Architecture for the MNIST-USPS dataset. (a) Best CNN architecture based on our validation procedure. (b) Results of some of our validation experiments to determine, which layers should not share weights and instead be connected by a regularization loss. The x -axis denotes the network configuration, where ‘+’ denotes that the weights of a particular layer are *not* shared, while ‘-’ means that they are.

vised setting, and thus ignore the target domain labels at training time. Following [32], as the image patches in the *USPS* dataset are only 16×16 pixels, we rescaled the images from *MNIST* to the same size and applied L_2 normalization of the gray-scale pixel intensities. For our tests, we rely on the standard CNN architecture of [34] and followed a similar validation procedure to that used for the previous two datasets to determine which layers should not share their weights. Specifically, as for the *Office* dataset, since there is no explicit validation set, we randomly sampled 5 images for each class from the target domain and used them to select the best network architecture. We found that allowing all layers of the network not to share their weights yielded the best performance. Fig. 8(a) depicts the final structure of the CNN. In Fig. 8(b), we provide the results of some of the validation experiments.

In Table 5, we compare our approach against other Domain Adaptation techniques. Our approach outperforms the baselines by a large margin. Overall we have compared our approach with various methods [30, 28, 7], which involve using deep architectures to extract domain invariant representations for both source and target domains. We further evaluated our approach with respect to methods [43, 18, 19, 42] that do not use deep networks. In all cases we believe that our method shows superior performance due to its ability to adapt the feature representation to each domain, while still keeping these representations close to each other.

method	Accuracy									
	NA	PCA	SA [19]	GFK [18]	TCA [43]	SSTCA [43]	TSL [44]	JCSL [42]	DDC [7]	Ours
M→U	0.454	0.451	0.486	0.346	0.408	0.406	0.435	0.467	0.478	0.607
U→M	0.333	0.334	0.222	0.226	0.274	0.222	0.341	0.355	0.631	0.673
AVG.	0.394	0.392	0.354	0.286	0.341	0.314	0.388	0.411	0.554	0.640

Table 5. Comparison against other domain adaptation techniques on the MNIST+USPS standard benchmark.

4.3 Discussion

In all the experiments reported above, allowing the weights *not* to be shared in at least some of the layers of our two-stream architecture boosts performance. This validates our initial hypothesis that explicitly modeling the domain shift is generally beneficial.

However the optimal choice of which layers should or should not share their weights is application dependent. In the UAV case, allowing the weights in the first two layers to be different yields top performance, which we understand to mean that the domain shift is caused by low-level changes that are best handled in the early layers. By contrast, for the *Office* dataset, it is best to only allow the weights in the last two layers to differ. This network configuration was determined using *Amazon* and *Webcam* images, such as those shown in Fig. 6. Close examination of these images reveals that the differences between them are not simply due to low-level phenomena, such as illumination changes, but to more complex variations. It therefore seems reasonable that the higher layers of the network should be domain-specific, since they typically encode this type of high-level information. Finally, for *MNIST+USPS*, it is optimal not to share any weights, which we take to be a consequence of the networks being relatively small and therefore requiring adaptation of all the parameters to provide sufficient flexibility.

Fortunately, we have shown that it is possible to use validation data to decide which configuration is best, which makes our two-stream approach a practical one.

5 Conclusion

In this paper, we have postulated that Deep Learning approaches to Domain Adaptation should not focus on learning features that are invariant to the domain shift, which makes them less discriminative. Instead we should explicitly model the domain shift. To prove this, we have introduced a two-stream CNN architecture, where the weights of the streams are not shared. To nonetheless encode the fact that both streams should be related, we encourage these weights to remain close to being linear transformations of each other by introducing an additional term in the loss function.

Our experiments have clearly validated our hypothesis. Our approach consistently yields higher accuracy than networks that share all weights for the source and target data. Furthermore, we have outperformed the state-of-the-art on three challenging object detection and recognition datasets involving both supervised and unsupervised scenarios. In the future, we intend to study if more complex weight transformations could help us improve our results, with a particular focus on designing effective constraints for the parameters of these transformations.

References

1. Hinton, G., Osindero, S., Teh, Y.: A Fast Learning Algorithm for Deep Belief Nets. *Neural Computation* **18** (2006) 1391–1415
2. LeCun, Y., Bottou, L., Orr, G., Müller, K.: *Efficient Backprop.* In: *Neural Networks: Tricks of the Trade.* Springer (1998)
3. Jiang, J.: *A Literature Survey on Domain Adaptation of Statistical Classifiers.* Technical report, University of Illinois at Urbana-Champaign (2008)
4. Pan, S., Yang, Q.: A Survey on Transfer Learning. *IEEE trans. on knowledge and data engineering* **22** (2010)
5. Girshick, R., Donahue, J., Darrell, T., Malik, J.: Rich feature hierarchies for accurate object detection and semantic segmentation. *arXiv Preprint* (2013)
6. Oquab, M., Bottou, L., Laptev, I., Sivic, J.: Learning and transferring mid-level image representations using convolutional neural networks. In: *CVPR.* (2014)
7. Tzeng, E., Hoffman, J., Zhang, N., Saenko, K., Darrell, T.: Deep Domain Confusion: Maximizing for Domain Invariance. *arXiv Preprint* (2014)
8. Long, M., Cao, Y., Wang, J., Jordan, M.I.: Learning Transferable Features with Deep Adaptation Networks. In: *International Conference on Machine Learning.* (2015)
9. Ganin, Y., Lempitsky, V.: Unsupervised Domain Adaptation by Backpropagation. In: *International Conference on Machine Learning.* (2015)
10. Tzeng, E., Hoffman, J., Darrell, T., Saenko, K.: Simultaneous Deep Transfer Across Domains and Tasks. In: *International Conference on Computer Vision.* (2015)
11. Duan, L., Tsang, I., D.Xu, Maybank, S.: Domain Transfer SVM for Video Concept Detection. In: *Conference on Computer Vision and Pattern Recognition.* (2009) 1375–1381
12. Bergamo, A., Torresani, L.: Exploiting weakly-labeled web images to improve object classification: a domain adaptation approach. In: *NIPS.* (2010)
13. Becker, C., Christoudias, M., Fua, P.: Non-Linear Domain Adaptation with Boosting. In: *Advances in Neural Information Processing Systems.* (2013)
14. H. Daumé, I., Marcu, D.: Domain Adaptation for Statistical Classifiers. *J. Artif. Int. Res.* **26**(1) (2006) 101–126
15. Saenko, K., Kulis, B., Fritz, M., Darrell, T.: Adapting Visual Category Models to New Domains. In: *European Conference on Computer Vision.* (2010) 213–226
16. Kulis, B., Saenko, K., Darrell, T.: What You Saw is Not What You Get: Domain Adaptation Using Asymmetric Kernel Transforms. In: *Conference on Computer Vision and Pattern Recognition.* (2011)
17. Gopalan, R., Li, R., Chellappa, R.: Domain Adaptation for Object Recognition: An Unsupervised Approach. In: *International Conference on Computer Vision.* (2011)
18. Gong, B., Shi, Y., Sha, F., Grauman, K.: Geodesic Flow Kernel for Unsupervised Domain Adaptation. In: *Conference on Computer Vision and Pattern Recognition.* (2012)
19. Fernando, B., Habrard, A., Sebban, M., Tuytelaars, T.: Unsupervised Visual Domain Adaptation Using Subspace Alignment. In: *International Conference on Computer Vision.* (2013)
20. Chopra, S., Balakrishnan, S., Gopalan, R.: DLID: Deep Learning for Domain Adaptation by Interpolating Between Domains. In: *International Conference on Machine Learning.* (2013)
21. Gretton, A., Borgwardt, K., Rasch, M., Schölkopf, B., Smola, A.: A Kernel Method for the Two-Sample Problem. *arXiv Preprint* (2008)
22. Huang, J., Smola, A., Gretton, A., Borgwardt, K., Schölkopf, B.: Correcting Sample Selection Bias by Unlabeled Data. In: *Advances in Neural Information Processing Systems.* (2006)
23. Gretton, A., Smola, A., Huang, J., Schmittfull, M., Borgwardt, K., Schölkopf, B.: Covariate Shift by Kernel Mean Matching. *Journal of the Royal Statistical Society* **3**(4) (2009) 5–13

24. Gong, B., Grauman, K., Sha, F.: Connecting the Dots with Landmarks: Discriminatively Learning Domain-Invariant Features for Unsupervised Domain Adaptation. In: International Conference on Machine Learning. (2013)
25. Pan, S., Tsang, I., Kwok, J., Yang, Q.: Domain Adaptation via Transfer Component Analysis. *IEEE Transactions on Neural Networks* **22**(2) (2011) 199–210
26. Muandet, K., Balduzzi, D., Schölkopf, B.: Domain Generalization via Invariant Feature Representation. In: International Conference on Machine Learning. (2013)
27. Baktashmotlagh, M., Harandi, M., Lovell, B., Salzmann, M.: Unsupervised Domain Adaptation by Domain Invariant Projection. In: International Conference on Computer Vision. (2013)
28. Ghifary, M., Kleijn, W.B., Zhang, M.: Domain Adaptive Neural Networks for Object Recognition. *arXiv Preprint* (2014)
29. Bay, H., Ess, A., Tuytelaars, T., Van Gool, L.: SURF: Speeded Up Robust Features. *Computer Vision and Image Understanding* **10**(3) (2008) 346–359
30. Donahue, J., Jia, Y., Vinyals, O., Hoffman, J., Zhang, N., Tzeng, E., Darrell, T.: DeCAF: A Deep Convolutional Activation Feature for Generic Visual Recognition. In: International Conference on Machine Learning. (2014)
31. Chopra, S., Hadsell, R., LeCun, Y.: Learning a Similarity Metric Discriminatively, with Application to Face Verification. In: Conference on Computer Vision and Pattern Recognition. (2005)
32. Long, M., Wang, J., Ding, G., Sun, J., Yu, P.: Transfer Feature Learning with Joint Distribution Adaptation. In: International Conference on Computer Vision. (2013) 2200–2207
33. Zeiler, M.D.: ADADELTA: an Adaptive Learning Rate Method. *Computing Research Repository* (2012)
34. LeCun, Y., Bottou, L., Bengio, Y., Haffner, P.: Gradient-Based Learning Applied to Document Recognition. *IEEE* (1998)
35. Krizhevsky, A., Sutskever, I., Hinton, G.: ImageNet Classification with Deep Convolutional Neural Networks. In: *Advances in Neural Information Processing Systems*. (2012)
36. Rozantsev, A., Lepetit, V., Fua, P.: On Rendering Synthetic Images for Training an Object Detector. *Computer Vision and Image Understanding* **137** (2015) 24–37
37. Jin, J., Fu, K., Zhang, C.: Traffic Sign Recognition with Hinge Loss Trained Convolutional Neural Networks. *IEEE Transactions on Intelligent Transportation Systems* **15** (2014) 1991–2000
38. Jaderberg, M., Simonyan, K., Zisserman, A., Kavukcuoglu, K.: Spatial Transformer Networks. *arXiv Preprint* (2015)
39. Li, W., Duan, L., Xu, D., Tsang, I.W.: Learning with Augmented Features for Supervised and Semi-Supervised Heterogeneous Domain Adaptation. *IEEE Transactions on Pattern Analysis and Machine Intelligence* (2014) 1134–1148
40. Tommasi, T., Caputo, B.: Frustratingly Easy NBNN Domain Adaptation. In: International Conference on Computer Vision. (2013)
41. Hull, J.: A Database for Handwritten Text Recognition Research. *IEEE Transactions on Pattern Analysis and Machine Intelligence* **16** (1994) 550–554
42. Fernando, B., Tommasi, T., Tuytelaars, T.: Joint Cross-Domain Classification and Subspace Learning for Unsupervised Adaptation. *Pattern Recognition Letters* **65** (2015) 60–66
43. Pan, S., Tsang, I., Kwok, J., Yang, Q.: Domain Adaptation via Transfer Component Analysis. In: International Joint Conference on Artificial Intelligence. (2009) 1187–1192
44. Si, S., Tao, D., Geng, B.: Bregman Divergence-Based Regularization for Transfer Subspace Learning. *IEEE Trans. Knowl. Data Eng.* **22**(7) (2010) 929–942